Journal of Experimental Botany, Vol. 62, No. 14, pp. 5161–5177, 2011
doi:10.1093/jxb/err221 Advance Access publication 15 July, 2011
This paper is available online free of all access charges (see http://jxb.oxfordjournals.org/open_access.html for further details)

Journal of Experimental Botany
www.jxb.oxfordjournals.org

RESEARCH PAPER

Arabidopsis CSLD1 and *CSLD4* are required for cellulose deposition and normal growth of pollen tubes

Wei Wang[1], Li Wang[1], Chen Chen[1], Guangyan Xiong[2], Xiao-Yun Tan[1], Ke-Zhen Yang[1], Zi-Chen Wang[1], Yihua Zhou[2], De Ye[1] and Li-Qun Chen[1,*]

[1] State Key Laboratory of Plant Physiology and Biochemistry, College of Biological Sciences, China Agricultural University, Beijing 100193, China
[2] Institute of Genetics and Developmental Biology, Chinese Academy of Sciences, Beijing 100101, China

* To whom correspondence should be addressed. E-mail: chenliqun@cau.edu.cn

Received 25 February 2011; revised 20 June 2011; Accepted 20 June 2011

Abstract

The cell wall is important for pollen tube growth, but little is known about the molecular mechanism that controls cell wall deposition in pollen tubes. Here, the functional characterization of the pollen-expressed *Arabidopsis* cellulose synthase-like D genes *CSLD1* and *CSLD4* that are required for pollen tube growth is reported. Both *CSLD1* and *CSLD4* are highly expressed in mature pollen grains and pollen tubes. The CSLD1 and CSLD4 proteins are located in the Golgi apparatus and transported to the plasma membrane of the tip region of growing pollen tubes, where cellulose is actively synthesized. Mutations in *CSLD1* and *CSLD4* caused a significant reduction in cellulose deposition in the pollen tube wall and a remarkable disorganization of the pollen tube wall layers, which disrupted the genetic transmission of the male gametophyte. In *csld1* and *csld4* single mutants and in the *csld1 csld4* double mutant, all the mutant pollen tubes exhibited similar phenotypes: the pollen tubes grew extremely abnormally both *in vitro* and *in vivo*, which indicates that *CSLD1* and *CSLD4* are not functionally redundant. Taken together, these results suggest that *CSLD1* and *CSLD4* play important roles in pollen tube growth, probably through participation in cellulose synthesis of the pollen tube wall.

Key words: *Arabidopsis*, cell wall, cellulose, *CSLD1*, *CSLD4*, pollen tube.

Introduction

In flowering plants, the pollen tube generated from the vegetative cell of the pollen grain is essential for delivery of male gametes to the female gametophyte in sexual reproduction (Hülskamp *et al.*, 1995; Johnson and Preuss, 2002; Lord and Russell, 2002). Studies have shown that biosynthesis of the pollen tube wall is involved in the regulation of pollen tube growth (Edlund *et al.*, 2004; Geitmann and Steer, 2006). Although it is important for pollen tube growth, the molecular mechanisms that control pollen tube wall biosynthesis remain largely unknown.

The pollen tube undergoes polar growth, namely the pollen tube elongates in one direction. Therefore, cell wall synthesis mainly occurs in the tip region of growing pollen tubes. The newly formed cell wall at the pollen tube tip is mainly composed of pectins, such as highly methylesterified homogalacturonan and rhamnogalacturonan I (Lancelle and Hepler, 1992; Edlund *et al.*, 2004; Geitmann and Steer, 2006; Dardelle *et al.*, 2010). This pectic layer continues along the entire length of the pollen tube and the homogalacturonans in this layer are gradually demethylesterified by pectin methylesterase (Lennon and Lord, 2000; Jiang *et al.*, 2005; Dardelle *et al.*, 2010). Behind the tip, a secondary layer is formed beneath the outer pectic fibrous layer (Ferguson *et al.*, 1998; Li *et al.*, 1999*a*). The most abundant component in this secondary wall layer is callose. Cellulose is also present in this layer, but at a low level (Dong *et al.*, 2005; Nishikawa *et al.*, 2005; Geitmann and Steer, 2006). For example, the pollen tube wall of *Nicotiana alata* contains only 5–10% cellulose (Schlüpmann *et al.*, 1994; Li *et al.*, 1999*a*), whereas the stem cell wall of

Arabidopsis thaliana contains 30% cellulose (Taylor *et al.*, 2003). Electron microscopy studies have shown that cellulose microfibrils in the pollen tube are thinner and shorter than those in somatic cells. In addition, linkage assays indicate that cellulose from pollen tubes is a heteropolymer containing β-1,4 linkages and a few β-1,3 linkages, rather than a homogeneous β-1,4-linked glucan (Steer and Steer, 1989; Geitmann and Steer, 2006). These findings imply that the cellulosic material of pollen tubes differs from that of somatic cells and that it more closely resembles cellulose from lower eukaryotes than that of the somatic cells of higher plants. Moreover, treatment with cellulase or specific inhibitors of cellulose biosynthesis severely represses pollen tube growth (Anderson *et al.*, 2002; Aouar *et al.*, 2010). Furthermore, the distribution of cellulose synthase (CESA) in pollen tubes depends on actin filaments and endomembrane dynamics, but does not depend on microtubules (Cai *et al.*, 2011), whereas movement of CESA in somatic cells is highly regulated by cortical microtubules (Crowell *et al.*, 2009). These results show that there probably exists a special mechanism for cellulose deposition in pollen tubes. So far, although many genes have been predicted to be involved in cellulose synthesis in somatic cells (Mutwil *et al.*, 2008), the genes responsible for cellulose synthesis in pollen tubes remain largely unknown.

In plant somatic cells, cellulose is synthesized by CESA at the plasma membrane (Kimura *et al.*, 1999; Richmond and Somerville, 2000; Taylor, 2008). *CESA* genes belong to a superfamily that also includes nine cellulose synthase-like (CSL) families (*CSLA*/*B*/*C*/*D*/*E*/*F*/*G*/*H*/*J*; Yin *et al.*, 2009). Apart from *CESA* genes, several *CSL* genes have also been shown to encode glycan synthases for hemicellulosic polysaccharides. For example, *CSLA* genes are involved in the formation of mannan (Dhugga *et al.*, 2004; Liepman *et al.*, 2005). *CSLC* genes encode enzymes that catalyse the elongation of the backbone of xyloglucan (Cocuron *et al.*, 2007). *CSLF* and *CSLH* genes are responsible for β-(1–3,1–4)-D-glucan synthesis (Burton *et al.*, 2006; Doblin *et al.*, 2009). Although the products of these *CSL* genes have been identified, the functions of the other *CSL* genes including the *CSLD* genes remain unknown. To date, several mutants with lesions in *CSLD* genes have been described. Most of these mutations affect the polar growth of root hairs, pollen tubes, or xylem (Favery *et al.*, 2001; Wang *et al.*, 2001; Bernal *et al.*, 2007, 2008; Kim *et al.*, 2007; Li *et al.*, 2009). For example, mutations in *Arabidopsis CSLD1* and *CSLD4* drastically impair pollen germination and pollen tube growth (Bernal *et al.*, 2008). However, how these two genes affect pollen tube growth and whether they are involved in cell wall deposition still remain unclear.

In this study, a detailed functional characterization of *CSLD1* and *CLSD4* was performed. The results show that mutations in *CSLD1* and *CLSD4* dramatically impair the deposition of cellulose in the pollen tube wall and lead to severe defects in pollen tube growth. In addition, it was found that CSLD1 and CSLD4 proteins display a polar localization at the plasma membrane at the tip of the growing pollen tube, which is highly similar to the characteristics of the CESAs functioning in somatic cells. These new findings suggest that *CSLD1* and *CLSD4* could play important roles in cellulose synthesis for pollen tubes.

Materials and methods

Plant materials and mutant isolation

Mutant and wild-type seeds were surface sterilized and pre-germinated on Murashige and Skoog (MS) medium (Murashige and Skoog, 1962) plates with or without 50 mg ml^{-1} of kanamycin (Sigma) at 22 °C under a photoperiod of 16 h light/8 h dark. The plants were grown in soil at 22 °C under the same light cycle as for pre-germination. The generation of transposon *dissociation* (*Ds*) insertion mutants, *csld4-2* and *csld4-3*, was performed as described by Sundaresan *et al.* (1995). The *csld1-1* seeds (SALK_043260; Bernal *et al.*, 2008) were obtained from the *Arabidopsis* Biological Resource Center (ABRC, www.arabidopsis.org), and the T-DNA insertion site was determined by PCR using the primer pair LBa1/D1-S1 (The sequences of all the primers used in this study are listed in Supplementary Table S2 available at *JXB* online). DNA preparation and Southern blotting were performed as described by Yang *et al.* (1999).

Phenotypic characterization

In vitro pollen tube growth assays were performed as described by Li *et al.* (1999*b*) with a small modification. Pollen grains from ~6 anthers were plated onto the surface of agar plates (3 mm×3 mm). The pollen grains spread on the agar plates were cultured immediately at 22 °C and 100% relative humidity for ~6 h and then visualized by light microscopy (Leitz DM2500; Leica, Wetzlar, Germany). For *in vivo* pollen growth assays, mature pistils of the male-sterile mutant *male sterility 1* (*ms1*; Zinkl *et al.*, 1999) were pollinated with a limited number (3–5) of pollen grains from the mutants and wild-type plants. The pollen tubes in the pistils were stained with aniline blue and viewed with a fluorescence microscope (Leitz DM2500) as described by Jiang *et al.* (2005) and Tan *et al.* (2010). 4',6-Diamidino-2-phenylindole (DAPI) staining was performed as described by McCormick (2004). Alexander staining was performed as described by Alexander (1969). β-Glucuronidase (GUS) staining was performed as described by Jia *et al.* (2009). For Calcofluor and Pontamine Fast Scarlet 4B (S4B; Sigma) staining (Hoch *et al.*, 2005; Anderson *et al.*, 2009), quartets were cultured *in vitro* at 16 °C for 12 h and then fixed and stained with Calcofluor and S4B as described by Anderson *et al.* (2009) and Dardelle *et al.* (2010). Specifically, 0.01% (w/v) S4B was dissolved in liquid pollen germination medium (without agar) instead of liquid half-strength MS medium. FM4-64 staining was performed as described by Szumlanski *et al.* (2009). Fluorescence recovery after photobleaching (FRAP) and brefeldin A (BFA) treatment were performed as described by Lee *et al.* (2008). Morphological observation of pollen grains and pollen tubes by scanning electronic microscopy (SEM; Hitachi, S-3400N) and transmission electronic microscopy (TEM; JEM1230) was carried out as described by Hülskamp *et al.* (1995).

Molecular cloning

Isolation of the flanking sequences adjacent to the *Ds* element by thermal asymmetric interlaced PCR (TAIL-PCR) (Liu *et al.*, 1995) was performed as described previously (Yang *et al.*, 2003). The insertion site was confirmed by PCR using the primer pair D4-Ds/Ds5-1.

Full-length *CSLD1* and *CSLD4* genomic DNA fragments were amplified by PCR using the primer pairs D4-F-AF/D4-FAR, D4-F-BF/D4-FBR, and D1-FAF/D1-FAR, D1-F-BF/D1-FBR, respectively. The resulting DNA fragments were cloned into a pMD-18 T-vector for sequencing. For complementation experiments, the full-length *CSLD1* and *CSLD4* genomic DNA fragments were subcloned into a pCAMBIA1300 vector (CAMBIA, http://www.cambia.org) and introduced into *csld4-2*, *csld4-3*, and *csld1-1* heterozygous plants using the *Agrobacterium*-mediated infiltration method (Clough and Bent, 1998). For *CSLD4*, the transformant plants were selected on MS plates containing 25 mg l^{-1} of hygromycin B (Roche) and 50 mg l^{-1} of kanamycin, and confirmed by PCR using the primer pair 1300HindIII/D4-P1. For *CSLD1*, the transformant plants were selected by hygromycin B and confirmed by PCR using primer pair 1300HindIII/D1-P1.

The 2 kb *CSLD4* promoter fragment was amplified by PCR with the primer pair D4-PF/D4-PR and subcloned upstream of the *GUS* reporter gene in the pCAMBIA1300 vector. *CSLD1* and *CSLD4* cDNAs were cloned using RT-PCR with the gene-specific primer pairs D1-CAF/D1-CAR, D1-CBF/D1-CBR, D4-CAF/D4-CAR, and D4-CBF/D4-CBR. These cDNA fragments were then subcloned to create an N-terminal fusion gene with the green fluorescent protein (GFP) coding sequence downstream of the *CSLD4* promoter in pCAMBIA1300.

Confocal microscopy

A Zeiss LSM510 META laser-scanning microscope (Carl Zeiss, http://www.zeiss.com) was used in the experiments. GFP signals were excited at 488 nm and emission was collected at 505–530 nm. ROOT AND POLLEN ARFGAP (Song *et al.*, 2006) (RPA)–DsRed2 was excited at 543 nm, and emission was collected at 585–615 nm.

Spinning disk microscopy

Images were taken using an OLYMPUS IX81 microscope (OLYMPUS) equipped with a Yokogawa CSU-X1 spinning disk and an Andor iXon DV887ESV-BV camera (Plateforme d'Imagerie Dynamique, Institut Pasteur, Paris, France). A 405, 488, or 561 nm laser was used for excitation, and emission was collected using band-pass 405/25, 488/25, and 561/25 filters for Calcofluor, GFP, and DsRed2, respectively. Time series were acquired at a frame rate of 1–20 frames s^{-1}.

Results

Isolation and genetic analysis of csld1 and csld4 mutants

The two novel *csld4* alleles used in this study, *csld4-2* and *csld4-3*, were isolated in a screen for m̲ale gametop̲hyte defective (*mgp*) mutants in *Arabidopsis* ecotype Landsberg *erecta* (L*er*). Isolation of the genomic flanking sequences adjacent to the 5' end of the *Ds* element in these mutants revealed that both *Ds* insertions were located in the third exon of gene *At4g38190*, which encodes cellulose synthase-like protein CSLD4. The *Ds* elements were inserted 3273 bp and 3318 bp downstream of the ATG start codon in *csld4-2* and *csld4-3*, respectively (Fig. 1A). The *csld4-2* and *csld4-3* mutants were found to exhibit identical phenotypes. Therefore, *csld4-3* was used in most of the further characterization of the gene. The T-DNA in *csld1-1* (SALK_043260) is located in the third exon of *CSLD1* (*At2g33100*), 1492 bp downstream of the start codon (Fig. 1A).

Genetic analysis of *csld4* mutant lines was performed using a kanamycin selection marker carried by the *Ds* element and of *csld1* mutant lines by PCR-aided genotyping (Table 1). The progeny from self-pollinated heterozygous *csld1* (*csld1-1*/+) and heterozygous *csld4* (*csld4-2*/+ and *csld4-3*/+) mutant plants all exhibited segregation ratios of ~1 with insertion, to 1 without insertion (Table 1). These results indicate that the *csld1* and *csld4* mutants were probably defective in gametophyte function. Reciprocal crosses between the mutants and wild-type plants were then performed. When *csld1-1*/+, *csld4-2*/+, or *csld4-3*/+ plants were used as recipients in crosses with wild-type pollen, ~50% of the resulting progeny contained the T-DNA or *Ds* insertions (Table 1). When wild-type plants were used as recipients in crosses with the mutant plants, none of the resulting offspring was identified as having the insertions (Table 1). Therefore, the *csld1-1*, *csld4-2*, and *csld4-3* mutations completely suppressed the genetic transmission of male gametophytes and had no discernible influence on female gametophyte function. Furthermore, no homozygous mutant plants could be obtained in these mutant lines; therefore, heterozygous mutant plants were used for further phenotypic characterization of the male gametophytes.

The csld1 and csld4 mutations severely repress pollen tube growth both in vitro and in vivo

For characterization of mutant phenotypes, *csld4-3* and *csld1-1* were introgressed into the *quartet1* (*qrt1*) mutant background (Preuss *et al.*, 1994). In a *qrt1* homozygous mutant background, the four microspores from a microsporocyte fail to separate after meiosis, but their functions are virtually unaffected (Preuss *et al.*, 1994; Rhee and Somerville, 1998). Half of the pollen grains produced by the heterozygous mutant plants are mutant and half are wild type. Therefore, a quartet produced by the *csld* heterozygous mutant plants contains two mutant pollen grains (*csld*) and two wild-type pollen grains (*CSLD*). Pollen morphology, nuclear division, and pollen viability of the mutant plants were examined by SEM, DAPI staining, and Alexander staining, respectively. No obvious defects in the four pollen grains in the mature quartets (n >30) from the *csld1*/+; *qrt1*/*qrt1* and *csld4*/+; *qrt1*/*qrt1* plants were found compared with those from *qrt1*/*qrt1* plants (Fig. 1B), indicating that the *csld1* and *csld4* mutations do not affect pollen grain formation.

Germination and growth of the mutant pollen tubes were also examined (Table 2). Under *in vitro* conditions, ~87.6% and 83.6% of wild-type Col and L*er* pollen grains, respectively, produced normal pollen tubes (Fig. 2A, D). In contrast, only 45.4% of pollen grains from *csld1-1*/+ plants (Col background) and 43.9% of pollen grains from *csld4-3*/+ (L*er* background) plants produced normal pollen tubes. A total of 47.1% and 45.5% of the pollen grains from *csld1-1*/+ and *csld4-3*/+ plants, respectively, ruptured just after germination (Fig. 2B, E), while only 6.9% of Col and 8.4% of the L*er* pollen grains ruptured after germination. The percentages of ungerminated pollen grains in the mutants were similar to those in wild-type plants (Table 2). Germination assays were also performed in the *qrt1* background (Table 3). In the control, ~20.2% and 6.2% of *qrt1*/*qrt1* quartets had three or four pollen grains that produced

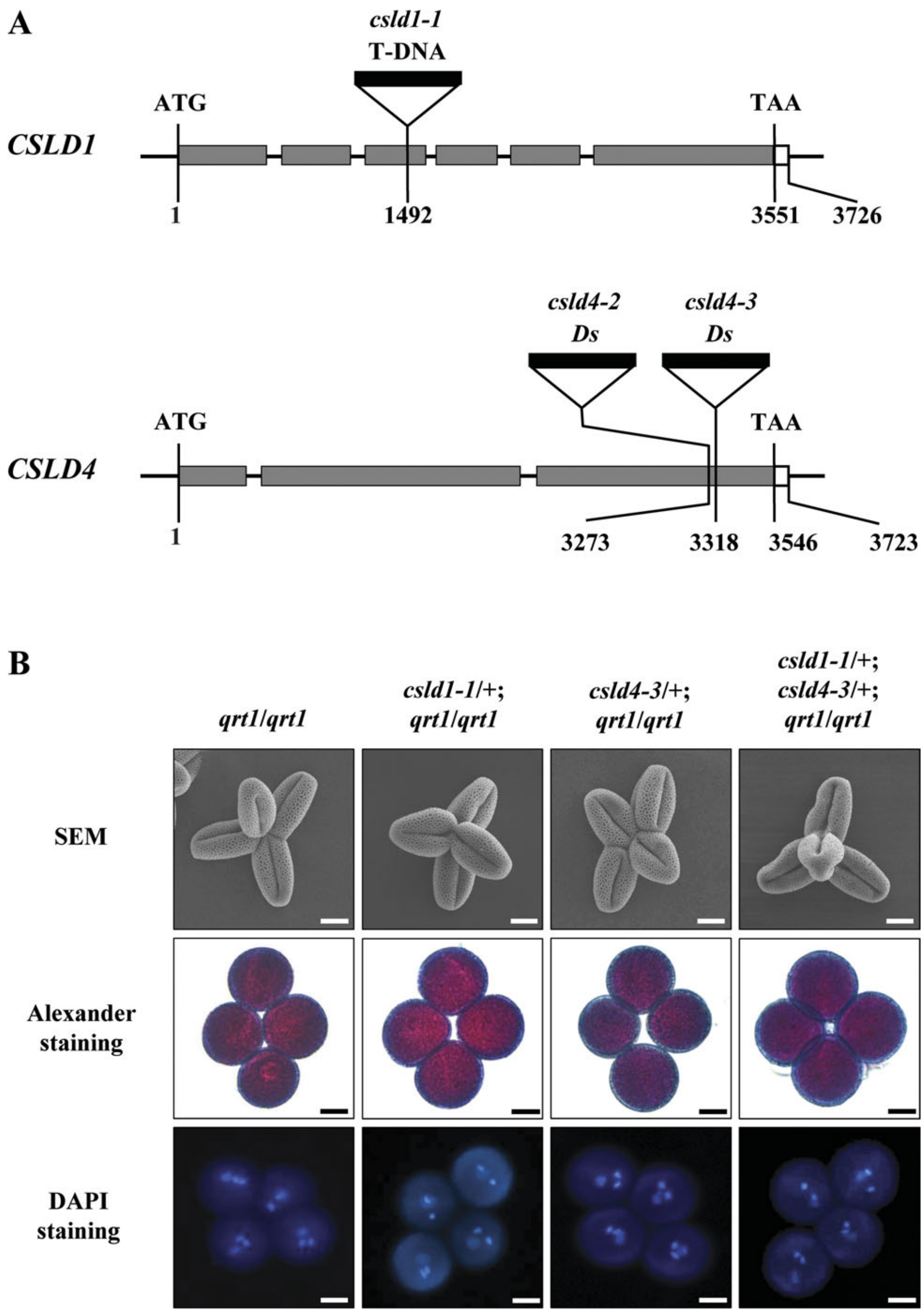

Fig. 1. Isolation of *CSLD1* and *CSLD4* knock-out mutants. (A) Schematic diagrams of the *CSLD1* and *CSLD4* gene structures, showing the T-DNA and *Ds* insertion sites. The grey and white boxes indicate translated and untranslated regions, respectively. (B) Scanning electron microscopy (SEM) analysis, Alexander staining, and DAPI staining of quartets from *qrt1/qrt1*, *csld1-1*/+; *qrt1/qrt1*, *csld4-3*/+; *qrt1/qrt1*, and *csld4-3*/+; *csld1-1*/+; *qrt1/qrt1*, respectively. For SEM analysis, pollen grains were coated with gold particles. Bars: 10 μm.

normal pollen tubes, respectively (Fig. 2G). In contrast, of the four pollen grains of each quartet from *csld1-1*/+; *qrt1/qrt1* and *csld4-3*/+; *qrt1/qrt1* mutant plants, a maximum of two produced normal pollen tubes; the rest ruptured just after germination or did not germinate (Fig. 2H–J).

Pollen germination was next investigated *in vivo* (see the Materials and methods). Most of the wild-type pollen grains produced normal pollen tubes (96% for Col, n=47; 95% for L*er*, n=108; Fig. 3A, B). In contrast, some of the pollen grains from *csld1*/+ (25%, n=146) or *csld4*/+ (27%, n=82) mutant plants produced abnormal pollen tubes after adhesion to the stigma. Some of the abnormal pollen tubes stopped growing in papillar cells (Fig. 3G–J), and some stopped growing in stigmas with expanded shapes (Fig. 3C–F). In summary, the *csld1* and *csld4* mutant pollen tubes were unstable and severely defective both *in vitro* and *in vivo*.

Table 1. *Genetic analysis of* csld4 *and* csld1 *mutants*

Crosses (female×male)	With insertion[a]	Without insertion[b]	Ratio	TE_F[c]	TE_M
csld4-2/+×csld4-2/+	368	361	1.02	NA	NA
csld4-3/+×csld4-3/+	516	529	0.98	NA	NA
csld4-2/+×Ler	1293	1314	0.98	100%	NA
csld4-3/+×Ler	1085	1052	1.03	100%	NA
Ler×csld4-2/+	0	1793	0.00	NA	0
Ler×csld4-3/+	0	1652	0.00	NA	0
csld1-1/+×csld1-1/+	62	61	1.02	NA	NA
csld1-1/+×Col	84	102	0.82	82%	NA
Col×csld1-1/+	0	180	0.00	NA	0%
Col×csld1-1/+; gD1/gD1[d]	55	40	1.38	100%	NA
Col×csld1-1/+; GFP-D1/GFP-D1	23	24	0.96	100%	NA
Col×csld1-1/+; GFP-D1/–	11[e]	21	0.52	52%	NA

[a] Kanamycin-resistant progeny in a *csld4-2* or *csld4-3* mutant background or progeny positive for the PCR analysis in the *csld1-1* mutant background.
[b] Kanamycin-sensitive progeny in a *csld4-2* or *csld4-3* mutant background or progeny negative for the PCR analysis in the *csld1-1* mutant background.
[c] TE, transmission efficiency; TE=(progeny with insertion/progeny without insertion)×100%; TE_F and TE_M, female and male transmission efficiency, respectively; NA, not applicable.
[d] *gD1* represents the *CSLD1* genomic DNA construct. *D1* represents *CSLD1*.
[e] All of these lines are associated with the *GFP-CSLD1* transgenic insertion.

Table 2. In vitro *germination of pollen grains from mutants, complemented mutants, and wild-type plants*

Pollen grains were cultured *in vitro* at 22 °C for 6 h. All results represent the average of three biological replicates with the standard deviation. For each independent replicate, at least 300 pollen grains were analysed.

Genotype	Germinated normally (%)	Ruptured (%)	Failed to germinate (%)
Col (+/+)	87.6±3.3	6.9±1.2	5.5±2.2
csld1-1/+	45.4±5.7	47.1±4.0	7.5±2.2
d1-1/d1-1; gD1/gD1	76.8±2.2	14.8±0.9	8.4±1.3
Ler (+/+)	83.6±3.4	8.4±2.5	8.0±0.9
csld4-3/+	43.9±1.4	45.5±0.7	10.6±0.9
d4-3/d4-3; gD4/gD4	78.5±1.7	15.2±1.5	6.3±1.1

Phenotypes of csld1 *and* csld4 *are rescued by wild-type* CSLD1 *and* CSLD4 *genes, respectively*

To confirm that the phenotypes of *csld4* and *csld1* were attributable to defects in *CSLD4* and *CSLD1*, respectively, complementation experiments were performed with the wild-type genomic DNAs and cDNAs of *CSLD4* and *CSLD1*. First, *CSLD4* and *CSLD1* genomic DNA fragments, including the predicted promoters, transcribed regions, and 3′ end non-transcribed regions, were cloned (*gCSLD4* and *gCSLD1*; see the Materials and methods) and introduced into *csld4* and *csld1* heterozygous plants. For *csld4*, 51 (in *csld4-2*) and 36 (in *csld4-3*) independent transformants were obtained in a screen; the progeny from 34 (in *csld4-2*) and 22 (in *csld4-3*) self-pollinated T_1 plants segregated in a ratio of ~2 kan^R to 1 kan^S (Supplementary Data File S1 at *JXB* online). For *csld1*, 12 independent transformants were obtained, and the plants heterozygous for *csld1-1* and homozygous for the transgenic *CSLD1* gene (*csld1-1*/+; *gCSLD1*/*gCSLD1*) in the T_2 generation were selected. These plants were used as the males in a cross with wild-type Col plants. Approximately 50% of the resulting F_1 seedlings carried the *csld1-1* T-DNA insertion (Table 1). Plants homozygous for both insertions and transgenic genes (*csld4*/*csld4*; *gCSLD4*/*gCSLD4* and *csld1-1*/ *csld1-1*; *gCSLD1*/*gCSLD1*) were obtained in the T_3 generation. The *in vitro* germination of pollen grains from the transgenic *csld4* homozygous plants was rescued from 43.9% to 78.5% (Fig. 2C, F; Table 2). In addition, expression of the N-terminal fusion of *CSLD4* and *CSLD1* with the *GFP*-encoding sequence driven by the *CSLD4* promoter (p*CSLD4:GFP-CSLD4* and p*CSLD4:GFP-CSLD1*) could also complement the phenotypes of *csld4* and *clsd1*, respectively (Tables 1, 4; Supplementary Data File S1). These results demonstrate that the phenotypes of *csld4* and *csld1* were caused by mutations in *CSLD4* and *CSLD1*, respectively.

The csld1 csld4 *double mutant shows no more severe defects*

To investigate whether *CSLD1* and *CSLD4* serve redundant functions, a *csld1 csld4* double mutant was generated. Because neither mutation can be transmitted through the male gametophyte, *csld1*/*csld1*; *GFP-CSLD1*/*GFP-CSLD1* transgenic plants were used as the males in a cross with *csld4-3*/+. F_1 plants with the *csld1*/+; *csld4*/+; *GFP-CSLD1*/– genotype were selected and self-pollinated. In the F_2 generation, the double-heterozygous mutant plants with the *csld1*/+; *csld4*/+ genotype that did not carry the transgenic *CSLD1* gene were selected (Supplementary Fig. S2 at *JXB* online). The *qrt1* mutation was also introgressed into the double mutant to generate *csld1*/+; *csld4*/+; *qrt1*/*qrt1* triple mutant plants. Because pollen grains in each quartet adhere to each other after meiosis, such plants produced three types of quartets: [2(*csld1 CSLD4*)+2(*CSLD1 csld4*)], [2(*CSLD1 CSLD4*)+2 (*csld1 csld4*)], and [(*csld1 CSLD4*)+(*CSLD1 csld4*)+(*CSLD1 CSLD4*)+(*csld1 csld4*)] (Supplementary Fig. S2). The (*csld1 csld4*) pollen grains represent the *csld1 csld4* double mutant pollen grains.

First, genetic analysis on *csld1*/+; *csld4*/+; *qrt1*/*qrt1* plants showed that neither *csld1* nor *csld4* could be transmitted through the male gametophyte, but that their transmission through the female gametophyte was not affected (Table 4). The construct p*CSLD4:GFP-CSLD4* was also introduced into the triple mutant. The results showed that expression of *GFP-CSLD4* in pollen could rescue the male transmission defects of *csld4* but not *csld1* pollen grains (Table 4).

Phenotypic analysis was then performed on quartets from *csld1*/+; *csld4*/+; *qrt1*/*qrt1* plants with regard to morphology, cytoplasmic density, or nuclear constitution, and no defects were observed (n >30; Fig. 1B). Pollen germination and tube growth of this triple mutant were further investigated *in vitro*. Theoretically, quartets with the genotype [2(*csld1 CSLD4*)+2(*CSLD1 csld4*)] should not have

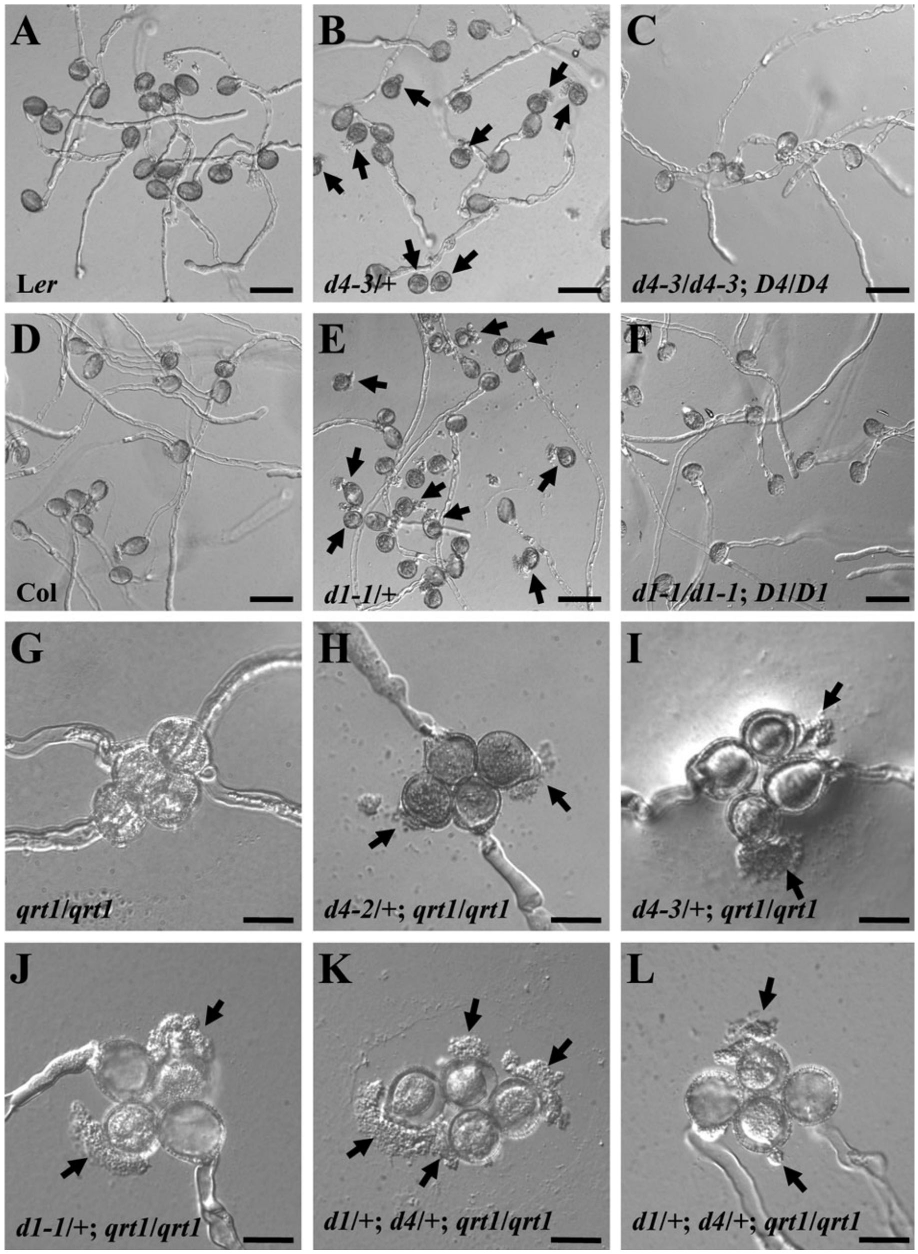

Fig. 2. *In vitro* germination of pollen grains from wild-type, mutant, and complemented mutant plants. Pollen grains were cultured *in vitro* at 22 °C for 6 h. (A–F) *In vitro* germination of pollen grains from L*er* (A), *csld4-3*/+ (B), complemented *csld4-3* (C), Col (D), *csld1-1*/+ (E), and complemented *csld1-1* (F) plants. Arrows indicate abnormal pollen tubes. (G–L) *In vitro* germination of quartets from *qrt1/qrt1* (G), *csld4-2*/+; *qrt1/qrt1* (H), *csld4-3*/+; *qrt1/qrt1* (I), *csld1-1*/+; *qrt1/qrt1* (J), and *csld4-3*/+; *csld1-1*/+; *qrt1/qrt1* (K, L) plants. Arrows indicate ruptured pollen tubes. *D1*, *D4*, *d1*, and *d4* represent *CSLD1*, *CSLD1*, *csld1*, and *csld4*, respectively. Bars: (A–F) 50 μm; (G–L) 20 μm.

produced any normal pollen tubes, quartets with the genotype [(*csld1 CSLD4*)+(*CSLD1 csld4*)+(*CSLD1 CSLD4*)+(*csld1 csld4*)] should have produced up to one normal pollen tube, and quartets with the genotype [2(*CSLD1 CSLD4*)+2(*csld1 csld4*)] should have produced up to two normal pollen tubes. It was observed that 45.5% (n=817) of the quartets from the triple mutant plants did not produce any normal pollen tubes (Fig. 2K, Table 3). Only 46.1% and 8.4% of the quartets (n=817) produced one or two normal pollen tubes (Fig. 2L; Table 3), respectively. The two pollen grains producing normal tubes in a quartet should be *CSLD1 CSLD4*, and the other two should be *csld1 csld4*; most of the latter (63.0%, n=216) ruptured after germination, like the *csld1* or *csld4* single mutant pollen grains (Supplementary Table S1 at *JXB* online). These results indicate that the phenotype of the the *csld1 csld4* double pollen grains was no more severe than that of the *csld1* and *csld4* single mutant pollen grains.

The structures of csld1 *and* csld4 *pollen tube cell walls are obviously disorganized*

To understand why the *csld1* and *csld4* mutant pollen grains ruptured easily after germination, the morphology

Table 3. In vitro *germination of quartets from wild-type and mutants plants*

Quartets were cultured *in vitro* at 22 °C for 6 h. All results represent the average of three biological replicates with the standard deviation. For each independent replicate, at least 200 quartets were analysed.

Genotype	No. of pollen grains germinated normally in a quartet				
	0 (%)	1 (%)	2 (%)	3 (%)	4 (%)
qrt1/qrt1	8.1±1.8	30.6±9.3	34.9±1.2	20.2±8.1	6.2±2.4
csld1-1/+; qrt1/qrt1	15.0±4.5	54.8±6.2	30.2±3.0	0.0	0.0
csld4-3/+; qrt1/qrt1	13.0±2.6	43.0±4.1	44.0±5.2	0.0	0.0
csld1-1/+; csld4-3/+; qrt1/qrt1	46.1±9.1	45.5±8.0	8.4±1.1	0.0	0.0

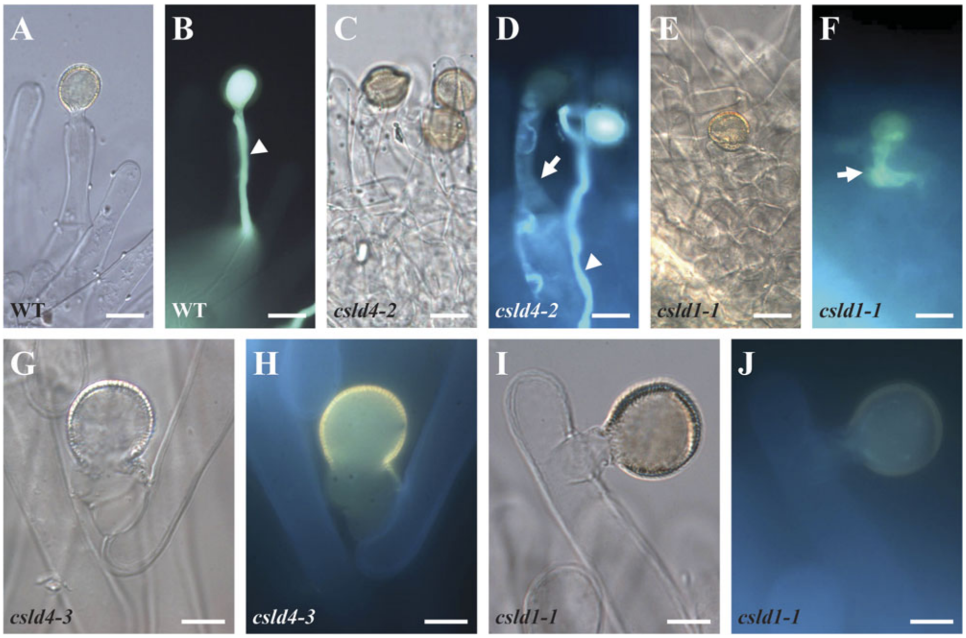

Fig. 3. *In vivo* germination of pollen grains from mutant and wild-type plants. *In vivo* germination of pollen grains from L*er* (A, B), *csld4*/+ (C, D, G, H), and *csld1-1*/+ (E, F, I, J) plants. Compared with wild-type pollen tubes, mutant pollen tubes were arrested at the surfaces of stigma cells (G–J) or expanded in the stigma (C–F). The white arrows indicate aberrant pollen tubes. The white arrowheads indicate normal pollen tubes. Bars: 20 μm.

Table 4. *Genetic analysis of the* csld1/+; csld4/+; qrt1/qrt1 *triple mutant*

Progeny were analysed by PCR in all of the crosses.

Crosses (female×male)	*D1/D1; D4/D4*	*d1/D1; D4/D4*	*D1/D1; d4/D4*	*d1/D1; d4/D4*	No. of F_1 seedlings
WT×*d1/D1; d4/D4*	100	0	0	0	100
d1/D1; d4/D4×WT	12	12	11	12	47
WT×*d1/D1; d4/D4; GFP-D4/–*	22	0	9[a]	0	31
d1/D1; d4/D4; GFP-D4/–×WT	12	5[b]	5	9[c]	31

[a] All these lines are associated with the *GFP-CSLD4* insertion.
[b] Four of the five lines are associated with the *GFP-CSLD4* insertion.
[c] Four of the nine lines are associated with the *GFP-CSLD4* insertion.

of the mutant pollen grains was examined using TEM. No obvious difference in surface appearance or cell wall structure was observed between mutant and wild-type pollen grains before germination (Supplementary Fig. S1 at *JXB* online). TEM images of the pollen grains germinated *in vitro* showed that newly emerging wild-type pollen tubes (*n*=18 for Col, *n*=19 for L*er*) had a characteristic cell wall consisting of an outer fibrous pectin layer and an inner non-fibrous callose layer (Fig. 4A–D), whereas about half of the pollen grains from *csld1*/+ and *csld4*/+ plants (five out of 11 for *csld1-1*/+, four out of 10 for *csld4-3*/+) produced pollen tubes that exhibited thickened and highly irregular cell walls (Fig. 4E–L). In particular, some of the *csld1* (Fig. 4I, J) and *csld4* (Fig. 4K, L) pollen grains produced pollen tubes without obvious non-fibrous materials in the wall (two out of 11 for *csld1-1*/+, two out of 10 for *csld4-3*/+) and blocks of fibrillar inclusions could be observed embedded inside the inner wall (Fig. 4F, H, J, L), which were probably caused by uneven deposition of cell wall polymers in the *csld1* and *csld4* pollen tube walls.

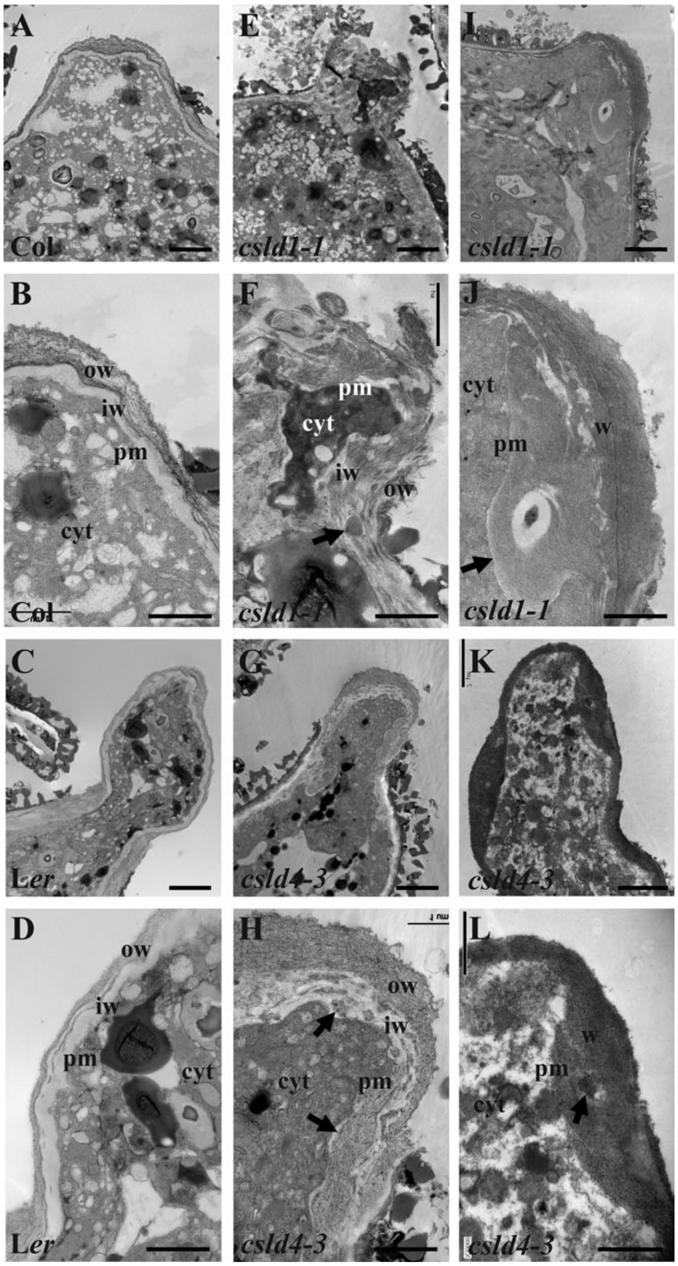

Fig. 4. Electronic microscopic observation of mutant and wild-type pollen tubes. Pollen grains were cultured *in vitro* at 16 °C for 3 h and then used for ultrathin sections. All of the ultrathin sections were stained with osmium tetroxide. Images show an overview of the newly emerging pollen tubes of Col (A), *csld1* (E, I), L*er* (C), and *csld4* (G, K), and high magnification of the cell wall of Col (B), *csld1* (F, J), L*er* (D), and *csld4* (H, L) pollen tubes. Wild-type Col (A, B) and L*er* (C, D) pollen tubes had a characteristic cell wall consisting of an outer fibrous pectin layer and an inner non-fibrous callose layer. Mutant pollen grains from *csld1*/+ (E–H) and *csld4*/+ (I–L) plants produced pollen tubes that exhibited thickened and highly irregular cell walls. Some of the *csld1* (I, J) and *csld4* (K, L) pollen grains produced pollen tubes without obvious non-fibrous materials in the tube wall. Arrows indicate blocks of fibrillar inclusions. ow, outer wall; iw, inner wall; w, wall; cyt, cytoplasm; pm, plasma membrane. Bars: (A, E, I, C, G and K) 2 μm; (B, F, J, D, H and L) 1 μm.

Both CSLD1 *and* CSLD4 *are highly expressed in mature pollen grains and pollen tubes*

To study the detailed expression patterns of *CSLD1* and *CSLD4*, transgenic lines transformed with the *GUS* gene driven by the *CSLD1* (CS70765) or *CSLD4* (CS70768) promoter from the ABRC were generated. GUS activity was detected in mature pollen and pollen tubes and was not detected in most other tissues/organs in these transgenic lines (Fig. 5; Supplementary Fig. S4 at *JXB* online). In p*CSLD1:GUS* transgenic lines, GUS activity was not detected in pollen until flower stage 12c and p*CSLD4:GUS* activity was not detected until flower stage 12b (Fig. 5). These data show that both *CSLD1* and *CSLD4* are specifically expressed in mature pollen and pollen tubes.

CSLD1 and CSLD4 are transported to the plasma membrane in the tip region of the pollen tube

As demonstrated above, p*CSLD4:GFP-CSLD1* and p*CSLD4:GFP-CSLD4* could complement the phenotypes of *csld1* and *csld4*, respectively, indicating that the N-terminal GFP fusion does not affect the normal function of CSLD1 and CSLD4. This suggests that the GFP fusion proteins probably present the correct localization of CSLD1 and CSLD4 *in vivo*. Accordingly, transgenic *Arabidopsis* lines expressing GFP–CSLD1 and GFP–CSLD4 were subjected to further analysis using confocal laser scanning microscopy (CLSM). The results showed that GFP–CSLD1 and GFP–CSLD4 are similarly located in pollen and pollen tubes. Before germination, GFP–CSLD1/4 (representing GFP–CSLD1 and GFP–CSLD4) exhibited punctate fluorescence signals in pollen grain cytoplasm, probably in the Golgi apparatus (Fig. 6A; Supplementary Fig. S5A at *JXB* online). To confirm this result, the GFP–CSLD1/4 plants were crossed with transgenic lines expressing the Golgi marker protein RPA (Song *et al.*, 2006; Deng *et al.*, 2010) with a C-terminal-fused red fluorescent tag, DsRed2, under the control of the pollen-specific *LAT52* promoter (RPA–DsRed2). In mature pollen grains, as shown in Fig. 6A and Supplementary Fig. S5A, the green fluorescence signals of GFP–CSLD1/4 showed the same localization pattern as the red fluorescence signals of RPA–DsRed2, indicating that CSLD1/4 products were indeed present in the Golgi apparatus before germination.

When the pollen grains began to germinate, the GFP–CSLD1/4 signals were found not only in the Golgi apparatus, but also in small vesicles, the cell periphery at the germinating point before emergence of the pollen tube (Fig. 6B; Supplementary Fig. S5B), and at the tip region of newly emerged (Fig. 6C; Supplementary Fig. S5C) and elongating (Fig. 6E; Supplementary Fig. S5E) pollen tubes where RPA–DsRed2 signals were absent. GFP–CSLD1/4 signals were also found at the periphery of the pollen tube plug (Fig. 6D; Supplementary Fig. S5D). To confirm that the GFP–CSLD1/4 signals on the cell periphery were located at the plasma membrane, the pollen tubes expressing GFP–CSLD4 were stained with the membrane-specific

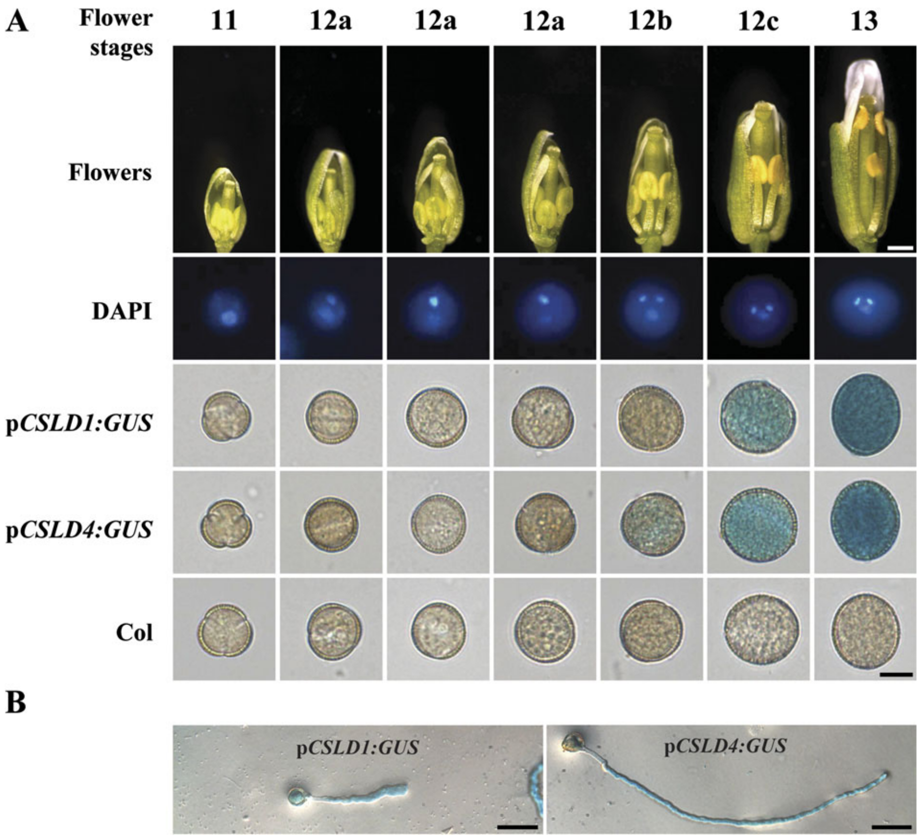

Fig. 5. Expression of *CSLD1* and *CSLD4* in pollen and pollen tubes. (A) Different stages of flowers (Smyth *et al.*, 1990) from p*CSLD1:GUS* and p*CSLD4:GUS* transgenic lines and wild-type plants were examined for GUS activity. Typical pollen grains with GUS staining are shown. (B) p*CSLD1:GUS* and p*CSLD4:GUS* pollen tubes showed GUS activity. Pollen grains were cultured *in vitro* at 22 °C for 6 h and then used for GUS staining. Bars: top of (A) 0.5 mm; bottom of (A) 10 μm; (B) 50 μm.

dye FM4-64 and it was found that the stain signals overlapped with the GFP–CSLD4 signals (Supplementary Fig. S6A at *JXB* online). Pollen tube plasmolysis also showed that GFP–CSLD1/D4 signals were localized to the plasma membrane (Supplementary Fig. S6B, C).

The above results show that GFP–CSLD1/4 proteins are likely to be associated with dynamic small vesicles exhibiting a characteristic 'V'-shaped pattern within the apical clear zone (Fig. 6E; Supplementary Fig. S5E and Videos S1, S2 at *JXB* online). The presence of vesicles arranged in this pattern is consistent with possible exocytosis and endocytosis at the apical region (Moscatelli and Idilli, 2009). To confirm whether GFP–CSLD1/4 proteins were inserted into the plasma membrane via exocytosis, FRAP was performed. The visible GFP–CSLD4 signals in the apical region of the cells, including those associated with the plasma membrane, were reduced to almost background levels after photobleaching. Recovery of the GFP–CSLD4 signals was first observed in the centre of the apical dome and then gradually appeared in the lateral region of the plasma membrane (10 independent experiments; Fig. 7A; Supplementary Video S3 at *JXB* online). The fluorescence fully recovered in the apical region of the plasma membrane ~30 s after photobleaching. In addition, plasma membrane localization of GFP-CSLD4 in the apical region was completely disrupted by BFA treatment (Fig. 7B, C). These results suggest that targeting of GFP–CSLD4 to the plasma membrane depends on exocytosis in the central region of the plasma membrane of the pollen tube tip. Based on these results, it is proposed that both CSLD1 and CSLD4 are preferentially located in the Golgi apparatus before germination and that during pollen germination and pollen tube growth they are transported to the plasma membrane at the tube tip via exocytosis.

csld1 *and* csld4 *pollen tube walls exhibit cellulose deficiencies*

To understand the roles of CSLD1 and CSLD4 in pollen tube growth, the effects of *csld1* and *csld4* mutations on the distribution of cell wall components in pollen tubes were investigated. Quartets from *qrt1*/*qrt1*, *csld1*/+; *qrt1*/*qrt1*, *csld4*/+; *qrt1*/*qrt1*, and *csld1*/+; *csld4*/+; *qrt1*/*qrt1* plants were cultured *in vitro* at 16 °C. As shown in Supplementary Fig. S3 at *JXB* online, *qrt1*/*qrt1* quartets produced up to four normal pollen tubes. Under the same conditions, up to two pollen grains in the *csld1* and *csld4* mutant quartets produced normal pollen tubes (representing wild-type); the other two pollen grains produced short and irregular pollen tubes (representing the mutant). These abnormal mutant pollen tubes were used for further analyses.

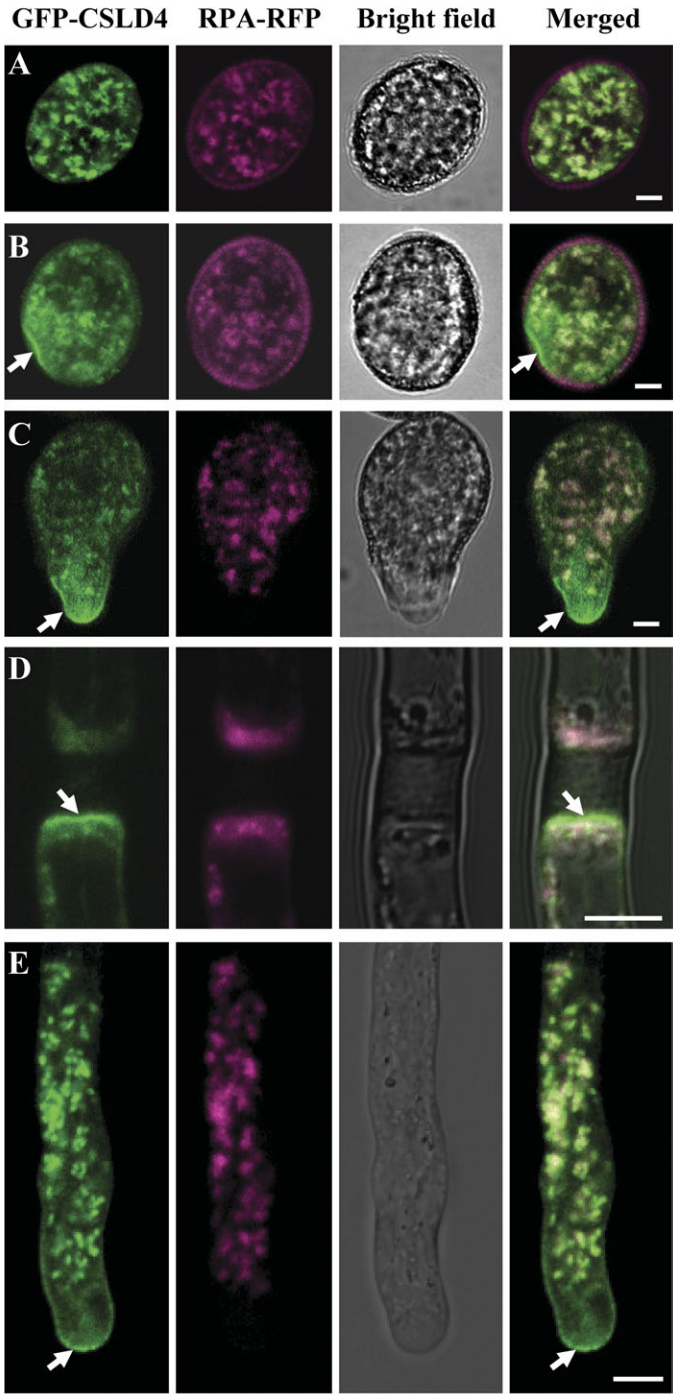

Fig. 6. Subcellular localization of CSLD4 *in vivo*. GFP–CSLD4 (green) co-localized with RPA–DsRed2 (magenta) in pollen grains before germination (A). GFP–CSLD4 signals were also observed at the cell periphery at the future pollen tube exit site (B, arrow) and at the plasma membrane of the freshly emerged pollen tube tip (C, arrow) and of growing pollen tubes (E, arrow). GFP–CSLD4 signals were also found at the plasma membrane adjacent to pollen tube plugs (arrow). Bars: 5 μm.

To investigate the distribution of β-glucans, such as callose and cellulose, in the mutant pollen tubes, cytochemical staining of the mutant pollen tubes with Calcofluor, aniline blue, and S4B was performed. Calcofluor stains both callose and cellulose (Sauter *et al.*, 1993; Dardelle *et al.*,

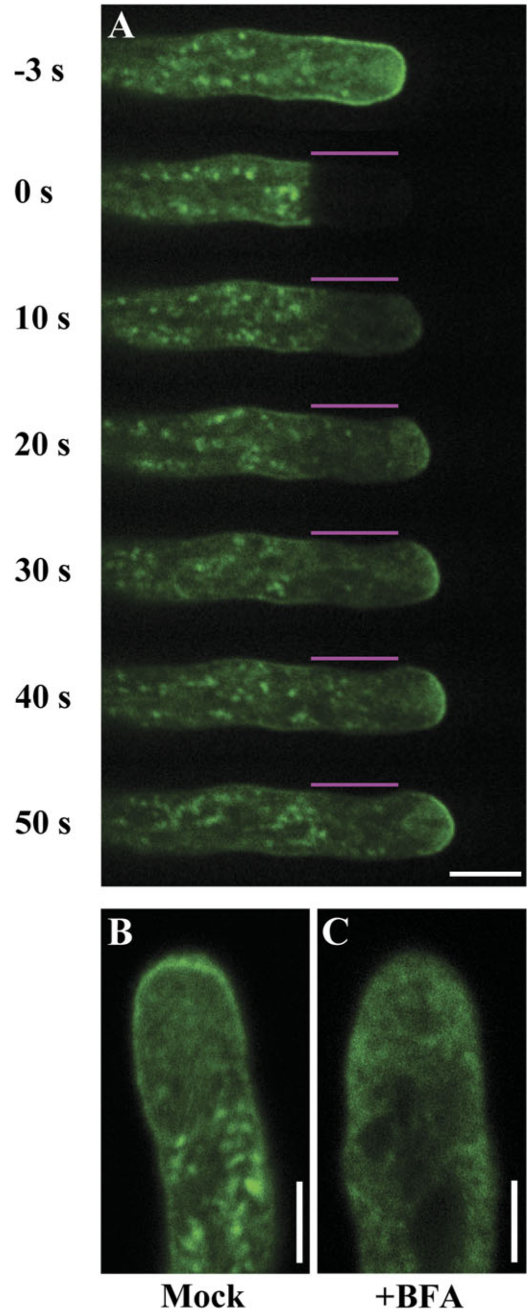

Fig. 7. FRAP analysis of GFP–CSLD4 in growing pollen tubes. Pollen grains were cultured *in vitro* at 22 °C for 6 h. (A) Spinning disk microscopy was used to perform FRAP in the tip region of growing pollen tubes expressing GFP–CSLD4. The fluorescence recovered at the plasma membrane of the pollen tube tip after photobleaching (10 independent experiments). Typically, a series of time-lapse images were taken every 10 s for 1 min. The numbers to the left of each image indicate elapsed time after photobleaching. The bleached area is marked by lines above the pollen tube. (B, C) Images showing pollen tubes expressing GFP–CSLD4 after mock treatment with 0.1% methanol (B), or treatment with 5 μg ml^{-1} BFA for 1 h (C). BFA completely disrupted the plasma membrane localization of GFP–CSLD4. Images were taken from the midplane. Bars: (A) 10 μm; (B, C) 5 μm.

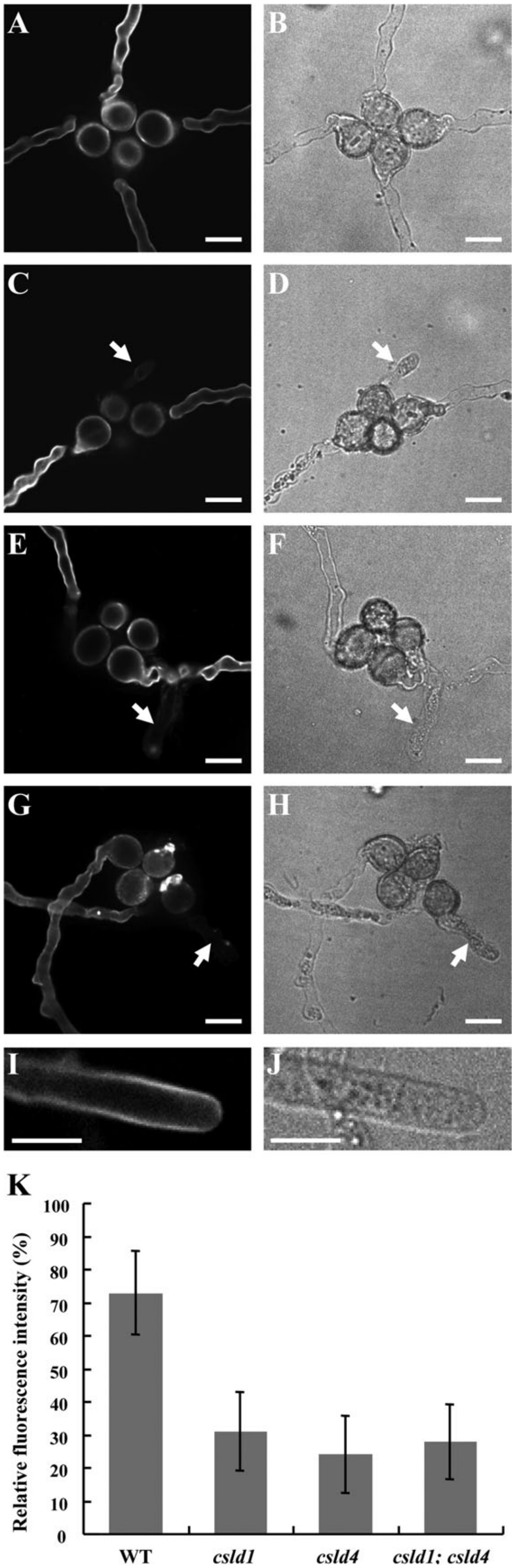

Fig. 8. Calcofluor staining of mutant and wild-type pollen tubes. Quartets were cultured *in vitro* at 16 °C for 12 h and then used for S4B staining. (A–H) Spinning disk confocal and bright field images of wild-type *qrt1/qrt1* (A, B), *csld4-3/+*; *qrt1/qrt1* (C, D), *csld1-1/+*; *qrt1/qrt1* (E, F), and *csld1-1/+*; *csld4-3/+*; *qrt1/qrt1* (G, H) pollen tubes stained with Calcofluor. Arrows indicate abnormal mutant pollen tubes. (I) and (J) Calcofluor staining of the tip region of a normal pollen tube, which cannot be shown in the same images above. (K) The fluorescence intensity of mutant pollen tubes was much weaker than that of control tubes. Images were taken at the same focal plane and the fluorescence intensity along the pollen tube wall was quantified by the grey value measured with ImageJ (Abramoff *et al.*, 2004; http://rsbweb.nih.gov/ij/). The fluorescence intensity of the brightest pollen tube was set to 100% and the weakest was measured (n=20 for wild-type *qrt1/qrt1*, n=26 for *csld1-1*, n=24 for *csld4-3*, and n=18 for the *csld1 csld4* double mutant). Bars: 20 μm.

2010). Aniline blue specifically stains callose, and S4B specifically stains cellulose (Hoch *et al.*, 2005; Anderson *et al.*, 2009). The Calcofluor-stained pollen tubes were observed using spinning disk microscopy. Most of the abnormal mutant pollen tubes showed almost no fluorescent signal (Fig. 8C, E, G). Only a few abnormal mutant pollen tubes (three of 26 for *csld1-1*, three of 24 for *csld4-3*, and two of 18 for the *csld1 csld4* double mutant) displayed punctate signals (Supplementary Fig. S7, D, H at *JXB* online) in comparison with the homogeneous signals of the control pollen tubes (Supplementary Fig. S7B). These signals may have been caused by the uneven deposition of cell wall materials that could be stained by Calcofluor. Thereafter, images were taken in the same focal plane and the fluorescence intensity along the pollen tube wall was measured with ImageJ (Abramoff *et al.*, 2004; http://rsbweb.nih.gov/ij/). Among pollen tubes of the same quartet, the pollen tube with the weakest fluorescence was compared with the tube showing the strongest fluorescence (Fig. 8K). The results showed that mutant pollen tube walls had much lower fluorescence intensity than did the control pollen tubes.

To examine the callose deposition in pollen tube walls, wild-type and mutant pollen tubes were stained with aniline blue. In wild-type pollen tubes, callose was mainly distributed in the tube shank region and was absent from the apical region of the elongated pollen tubes (Supplementary Fig. S8A, B at *JXB* online). The distribution of callose staining along *csld4* mutant pollen tubes was highly irregular (Supplementary Fig. S8C–J). In particular, 15 out of 21 *csld4* pollen tubes observed exhibited that the intensity of callose staining in the mutant pollen tube walls was weaker than that in the normal pollen tubes (Supplementary Fig. S8C–F), and six out of 21 *csld4* pollen tubes observed showed that callose was unevenly accumulated (Supplementary Fig. S8G–J). These results indicated that *csld4* mutation affected the deposition of callose in pollen tube walls.

Accordingly, S4B staining was used to investigate the content and distribution of cellulose in wild-type and mutant pollen tube walls. Although S4B staining of the cytoplasm of both mutant and wild-type pollen tubes was intense, there was a marked decrease in the intensity of S4B fluorescence in the cell wall of *csld1* (Fig. 9E, F), *csld4* (Fig. 9C, D), and *csld1 csld4* double mutant (Fig. 9G, H) pollen tubes

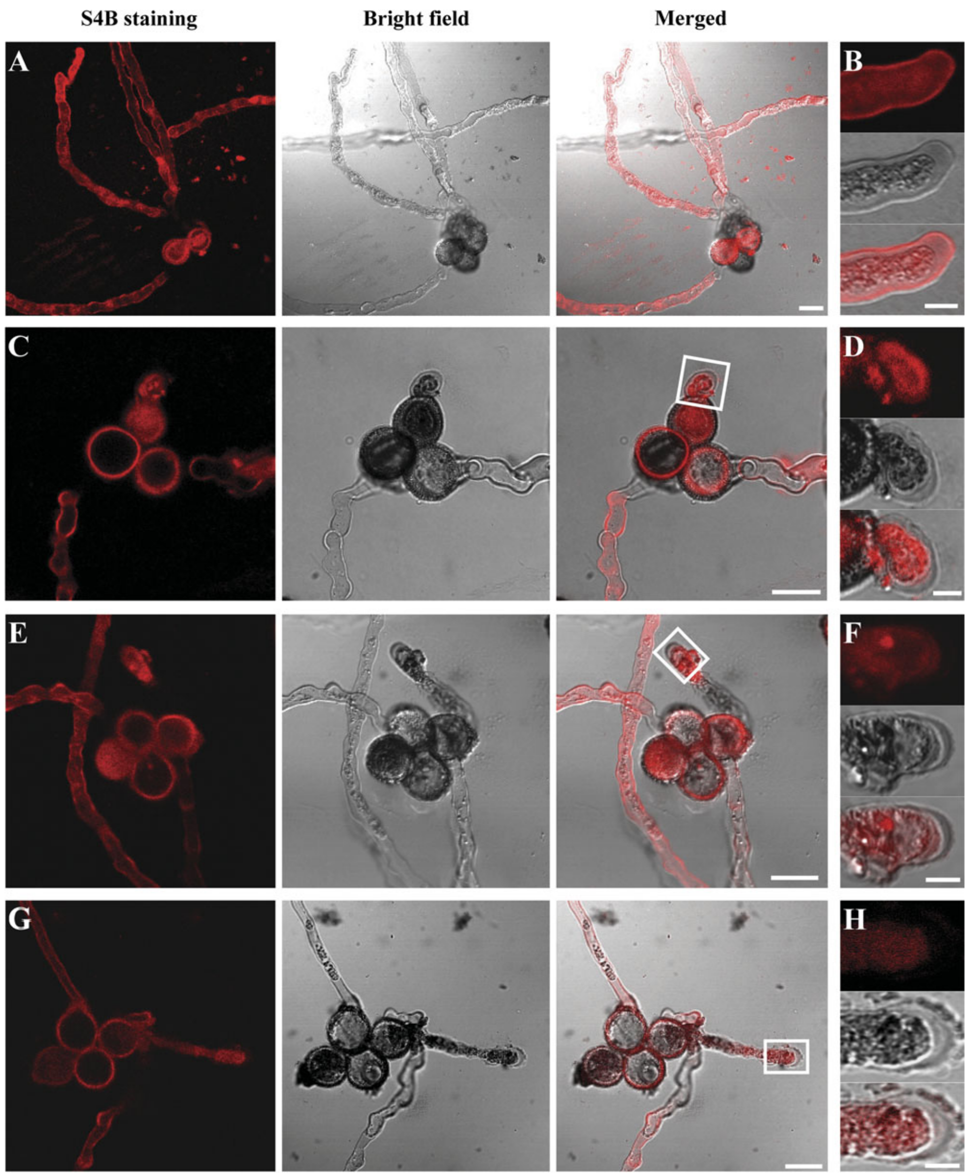

Fig. 9. S4B staining of mutant and wild-type pollen tubes. Confocal sections of wild-type *qrt1/qrt1* (A, B), *csld4-3/+*; *qrt1/qrt1* (C, D), *csld1-1/+*; *qrt1/qrt1* (E, F), and *csld1-1/+*; *csld4-3/+*; *qrt1/qrt1* (G, H) pollen tubes stained with S4B. The S4B fluorescence intensity in the cell wall of *csld4* (C, D), *csld1* (E, F), and *csld1 csld4* double mutant (G, H) pollen tubes was much weaker than that of wild-type pollen tubes (A, B). It is noteworthy that the S4B staining is weak at some parts of the pollen tube that are out of the focal planes shown here (especially the pollen tube base near the pollen grain). (B) High magnification image of a wild-type pollen tube showing S4B staining associated with the tube wall and cytoplasm. D, F, and H correspond to the white boxes in C, E, and G, respectively, showing that fluorescence was difficult to detect in the mutant pollen tube wall (five independent observations). Bars: (A, C, E, G) 20 μm; (B, D, F, H) 50 μm.

compared with that of wild-type pollen tubes (Fig. 9A, B), especially in the pollen tube tip (five independent observations). These results suggest that the cellulose content was significantly reduced in the mutant pollen tube walls.

Discussion

In this study, a detailed characterization of several mutant alleles of the *Arabidopsis CSLD1* and *CSLD4* genes was performed. The results show that these mutations disrupt pollen tube growth and reduce the cellulose content of the pollen tube walls. It was also found that the CSLD1 and CSLD4 proteins are transported to the plasma membrane of the pollen tube tip region during pollen germination and tube growth. Taken together, these results suggest that *CSLD1* and *CSLD4* play important roles in pollen tube growth, possibly by participating in pollen tube cellulose synthesis.

A regular framework of cellulose microfibrils is required for the deposition of other cell wall polymers such as callose and pectins. Disruption of this framework can result in thickening and irregularities in the cell wall (Persson *et al.*, 2007). Studies have shown that reduction or lack of cellulose in pollen tubes leads to severe defects in tube growth (Anderson *et al.*, 2002; Aouar *et al.*, 2010). Here it is shown that growth of *csld1* or *csld4* mutant pollen tubes is severely defective; moreover, the deposition of cellulose in the mutant pollen tubes is significantly reduced and the deposition of other cell wall polymers such as callose is irregular. This strongly implies that CSLD1 and CSLD4 may be involved in cellulose synthesis during pollen tube growth. This hypothesis is also supported by the following three observations.

First, both *CSLD1* and *CSLD4* encode putative CSLD proteins that, among the CSLs, share the highest sequence similarity to CESAs. Together with CSLFs, CSLDs and CESAs are closely phylogenetically related to each other and form a special category within the cellulose synthase superfamily (Yin *et al.*, 2009). CESAs are β-1,4-d-glucan (cellulose) synthases and CSLFs are β-(1–3,1–4)-d-glucan (MLG) synthases (Yin *et al.*, 2009). Accordingly, CSLDs have a high potential to be β-linked glucan synthases functioning as β-1,4-d-glucan synthases or β-(1–3,1–4)-d-glucan synthases.

Secondly, *CSLD1* and *CSLD4* are expressed abundantly in mature pollen and pollen tubes. To date, most *CSLD* genes have been found to be highly expressed in tip growing cells, while *CESA* genes are expressed at much lower levels in these cells. For example, tobacco pollen tubes express *CSLD* genes but do not express detectable *CESA* genes (Doblin *et al.*, 2001). In *Arabidopsis*, published microarray analyses (http://www.arabidopsis.org) and the results of the present study show that expression of *CSLD1* and *CSLD4* cannot be detected until the tricellular stage and that their expression increases significantly during pollen maturation and pollen tube growth. In contrast, in mature pollen and pollen tubes, the expression levels of all *CESA* genes are much lower than those of *CSLD1* and *CSLD4* (Honys and Twell, 2003, 2004; Qin *et al.*, 2009; this work, see Supplementary Data File S2 at *JXB* online). In the moss *Physcomitrella patens*, *CSLD* family members are most highly represented among *P. patens CESA* superfamily expressed sequence tags (ESTs), especially in cultures containing only protonemata that are undergoing tip growth (Roberts and Bushoven, 2007). These results indicate that *CSLD* genes are predominantly expressed in tip growing cells, in which *CESA* genes are present at low levels. Moreover, the *CESA* and *CSL* genes are reported to have distinct spatiotemporal expression patterns and may have distinct functions (Hamann *et al.*, 2004). Therefore, CSLDs may function as special cellulose synthases for tip growing cells.

Thirdly, the location of CSLD1 and CSLD4 within cells is consistent with their having a role in cellulose deposition in pollen tubes. Previous studies used transient expression of CSLD N-terminal fluorescently tagged fusion proteins in tobacco leaves (Bernal *et al.*, 2007, 2008; Li *et al.*, 2009) or proteomic analysis of *Arabidopsis* cellular compartments (Dunkley *et al.*, 2006) have shown that CSLDs are located in the Golgi apparatus. In this study, the recombinant p*CSLD4:GFP-CSLD1/4* constructs could successfully complement the mutant phenotype, indicating that GFP–CSLD1/4 fusion proteins were correctly targeted to the appropriate intracellular locations. The results showed that CSLD1/4 move from the Golgi apparatus to the plasma membrane by vesicle transport. The CSLD protein has also been identified in the plasma membrane proteome in rice (Natera *et al.*, 2008). The plasma membrane localization of CSLD1/4 is consistent with the known location of cellulose biosynthesis within the cell (Taylor, 2008) and with the phenotype of the mutant pollen tubes which exhibit defective pollen tube growth and reduction of cellulose deposition in the pollen tube wall (this study). The fusion proteins were also detected at the plasma membrane adjacent to the pollen tube plugs, where cellulose is also deposited (Ferguson *et al.*, 1998).

In addition, the localization pattern observed for CLSD1/4 in pollen tubes is similar to that of CESAs in somatic cells. Previous electron microscopic and proteomic analysis studies have shown that CESAs are located in both the plasma membrane and the Golgi apparatus (Haigler and Brown, 1986; Kimura *et al.*, 1999; Dunkley *et al.*, 2006; Natera *et al.*, 2008). Recent observations also show that fluorescent-tagged CESA3 and CESA6 move from the Golgi apparatus to the plasma membrane via vesicle exocytosis (Paredez *et al.*, 2006; Crowell *et al.*, 2009). Thus, the localization and movement of CESAs are consistent with their role as cellulose synthases in somatic cells. At the present time, it is not known if CESAs participate in cellulose biosynthesis of pollen tubes or not. To address the question, N-terminal GFP fusions of *Arabidopsis* CESA3 and CESA8 were expressed under the control of the *CSLD4* promoter in pollen tubes. The results showed that expression of CESA3 and CESA8 in pollen grains and pollen tubes could not complement the *csld1* and *csld4* mutants, implying that the CESAs could not replace the functions of CLSD1 and CLSD4 in pollen tubes. In addition, GFP–CESA3 and GFP–CESA8 expressed in pollen tubes are located in the Golgi apparatus, but not in the vesicles or plasma membrane of the pollen tube tip (Supplementary Fig. S10 at *JXB* online). Based on immunofluorescence microscopy data, it was recently reported that CESA proteins localize to the plasma membrane at the tip of *Nicotiana alata* pollen tubes (Cai *et al.*, 2011). However, the CESA antibody used in this study was generated against a peptide sequence that has high similarity (with identities of 85%) to NaCSLD1 (AAK49455.1) identified in *N. alata* pollen tubes (Cai *et al.*, 2011). Beside this, *CESA* genes are not expressed detectably in *N. alata* pollen tubes, while *NaCSLD1* is highly expressed (Doblin *et al.*, 2001). These CESA localization data can therefore not rule out the possibility that CSLD proteins are located in the plasma membrane of the pollen tube tip and CESAs are not. Taken together, the present data imply that CSLDs may be involved in the synthesis of cellulose at the tip region of the pollen tube and that CESAs may not be involved in this process. Thus, CSLD1 and CSLD4 may be specifically involved in biosynthesis of cellulose in growing pollen tubes. Nevertheless, the actual mechanisms that control cellulose synthesis in pollen tubes and somatic cells remain unknown. Further study is required to address this question.

CESAs from land plants and some algae assemble into hexagonal arrangements known as 'rosettes' or terminal complexes (TCs) (Tsekos, 1999; Roberts and Roberts, 2007; Taylor, 2008). This raises the interesting question of whether CSLD1 and CSLD4 also function in a complex. Indeed, TCs have been described in many tip growing cells including pollen tubes (Wada and Staehelin, 1981; Emons, 1985; Reiss *et al.*, 1985; Tsekos and Reiss, 1994). In most tip growing cells, the density of TCs is high in the tip region and decreases toward the base of the cell, a distribution that is consistent with the polar localization of CSLD1 and CSLD4 in pollen tubes observed in this study. In addition, although *CSLD1* and *CSLD*4 have similar expression patterns, *csld1* and *csld4* single mutants, as well as the *csld1 csld4* double mutant, have similar phenotypes even at lower temperature. The phenotype of the *csld1* mutant could not be complemented by the p*CSLD4:GFP-CSLD4* construct that could complement the phenotype of the *csld4* mutants (Table 4). These results suggest that CSLD1 and CSLD4 are not functionally redundant and that they probably function as a complex in cellulose synthesis. The N-terminal portions of CESAs contain Zn-binding domains that are proposed to serve in CESA–CESA interactions (Kurek *et al.*, 2002). CSLD4 and most of the other CSLDs have similar Zn-binding domains near the N-terminus, but CSLD1 does not have the domain (Supplementary Fig. S9 at *JXB* online) (Doblin *et al.*, 2001). Moreover, thus far, attempts to address this question have failed to achieve any conclusive results. Whether CSLD1 and CSLD4 assemble into TCs remains unknown, representing an interesting question to be addressed further.

Supplementary data

Supplementary data are available at *JXB* online.

Figure S1. TEM observation of mutant pollen grains before germination.

Figure S2. Generation of *csld1 csld4* double mutants.

Figure S3. *In vitro* germination of quartets from mutant and wild-type plants at different temperatures.

Figure S4. Expression patterns of *CSLD1* and *CSLD4*.

Figure S5. Subcellular localization of CSLD1 in *Arabidopsis* pollen grains and pollen tubes.

Figure S6. GFP–CSLD1 and GFP–CSLD4 are located at the plasma membrane of the pollen tube tip.

Figure S7. Calcofluor staining of wild-type and mutant pollen tubes.

Figure S8. Callose distribution in wild-type and mutant pollen tubes.

Figure S9. Homology of the predicted amino acid sequences of the CSLD and CESA proteins.

Figure S10. Subcellular localization of CESA3 and CESA8 in *Arabidopsis* pollen tubes.

Table S1. Primers used for cloning and PCR assays.

Table S2. *In vitro* germination of quartets from mutants and wild-type plants.

Videos S1. and S2. GFP–CSLD1 (Video S1) and GFP–CSLD4 (Video S2) move in pollen tubes.

Video S3. FRAP analysis of GFP–CSLD4 in the pollen tube tip of growing pollen tubes.

Data File S1. Genetic analysis of *CSLD4* transgenic *csld4* mutant lines.

Data File S2. Expression levels of *CESA* and *CSLD* genes during pollen development.

Acknowledgements

We thank Dr V. Sundaresan, Dr Wei-Cai Yang, and Ms Li-Fen Xie for their kind help with the mutant screens. We also thank Dr Youqun Wang for assistance with TEM analysis, and undergraduate students Yi Wang and Jilong Wang for their assistance with genetic analysis and molecular cloning. This work was supported by research grants from the Natural Science Foundation of China (grant nos 30770133, J0730639); the Ministry of Sciences and Technology (grant nos 2007CB947603, 2007CB108700); and the Ministry of Education, PR China (grant no. B06003).

References

Abramoff MD, Magalhaes PJ, Ram SJ. 2004. Image processing with ImageJ. *Biophotonics International* **11,** 36–42.

Alexander MP. 1969. Differential staining of aborted and non-aborted pollen. *Stain Technology* **44,** 117–122.

Anderson CT, Carroll A, Akhmetova L, Somerville C. 2009. Real-time imaging of cellulose reorientation during cell wall expansion in *Arabidopsis* roots. *Plant Physiology* **152,** 787–796.

Anderson JR, Barnes WS, Bedinger P. 2002. 2,6-Dichlorobenzonitrile, a cellulose biosynthesis inhibitor, affects morphology and structural integrity of petunia and lily pollen tubes. *Journal of Plant Physiology* **159,** 61–67.

Aouar L, Chebli Y, Geitmann A. 2010. Morphogenesis of complex plant cell shapes: the mechanical role of crystalline cellulose in growing pollen tubes. *Sexual Plant Reproduction* **23,** 15–27.

Bernal AJ, Jensen JK, Harholt J, *et al*. 2007. Disruption of *ATCSLD5* results in reduced growth, reduced xylan and homogalacturonan synthase activity and altered xylan occurrence in *Arabidopsis*. *The Plant Journal* **52,** 791–802.

Bernal AJ, Yoo CM, Mutwil M, Jensen JK, Hou G, Blaukopf C, Sorensen I, Blancaflor EB, Scheller HV, Willats WG. 2008. Functional analysis of the cellulose synthase-like genes *CSLD1, CSLD2*, and *CSLD4* in tip-growing *Arabidopsis* cells. *Plant Physiology* **148,** 1238–1253.

Burton RA, Wilson SM, Hrmova M, Harvey AJ, Shirley NJ, Medhurst A, Stone BA, Newbigin EJ, Bacic A, Fincher GB. 2006. Cellulose synthase-like *CslF* genes mediate the synthesis of cell wall (1,3;1,4)-β-D-glucans. *Science* **311,** 1940–1942.

Cai G, Faleri C, Del Casino C, Emons AMC, Cresti M. 2011. Distribution of callose synthase, cellulose synthase, and sucrose synthase in tobacco pollen tube is controlled in dissimilar ways by actin filaments and microtubules. *Plant Physiology* **155,** 1169–1190.

Clough SJ, Bent AF. 1998. Floral dip: a simplified method for Agrobacterium-mediated transformation of *Arabidopsis thaliana*. *The Plant Journal* **16,** 735–743.

Cocuron JC, Lerouxel O, Drakakaki G, Alonso AP, Liepman AH, Keegstra K, Raikhel N, Wilkerson CG. 2007. A gene from the cellulose synthase-like C family encodes a β-1,4 glucan synthase. *Proceedings of the National Academy of Sciences, USA* **104,** 8550–8555.

Crowell EF, Bischoff V, Desprez T, Rolland A, Stierhof YD, Schumacher K, Gonneau M, Hofte H, Vernhettes S. 2009. Pausing of Golgi bodies on microtubules regulates secretion of cellulose synthase complexes in *Arabidopsis*. *The Plant Cell* **21,** 1141–1154.

Dardelle F, Lehner A, Ramdani Y, Bardor M, Lerouge P, Driouich A, Mollet JC. 2010. Biochemical and immunocytological characterizations of Arabidopsis pollen tube cell wall. *Plant Physiology* **153,** 1563–1576.

Deng Y, Wang W, Li WQ, Xia C, Liao HZ, Zhang XQ, Ye D. 2010. *MALE GAMETOPHYTE DEFECTIVE 2,* encoding a sialyltransferase-like protein, is required for normal pollen germination and pollen tube growth in *Arabidopsis*. *Journal of Integrative Plant Biology* **52,** 829–843.

Dhugga KS, Barreiro R, Whitten B, *et al*. 2004. Guar seed β-mannan synthase is a member of the cellulose synthase super gene family. *Science* **303,** 363–366.

Doblin MS, De Melis L, Newbigin E, Bacic A, Read SM. 2001. Pollen tubes of *Nicotiana alata* express two genes from different β-glucan synthase families. *Plant Physiology* **125,** 2040–2052.

Doblin MS, Pettolino FA, Wilson SM, Campbell R, Burton RA, Fincher GB, Newbigin E, Bacic A. 2009. A barley cellulose synthase-like CSLH gene mediates (1,3;1,4)-β-D-glucan synthesis in transgenic *Arabidopsis*. *Proceedings of the National Academy of Sciences, USA* **106,** 5996–6001.

Dong X, Hong Z, Sivaramakrishnan M, Mahfouz M, Verma DP. 2005. Callose synthase (CalS5) is required for exine formation during microgametogenesis and for pollen viability in *Arabidopsis*. *The Plant Journal* **42,** 315–328.

Dunkley TP, Hester S, Shadforth IP, *et al*. 2006. Mapping the *Arabidopsis* organelle proteome. *Proceedings of the National Academy of Sciences, USA* **103,** 6518–6523.

Edlund AF, Swanson R, Preuss D. 2004. Pollen and stigma structure and function: the role of diversity in pollination. *The Plant Cell* **16 Suppl,** S84–S97.

Emons AMC. 1985. Plasma-membrane rosettes in root hairs of *Equisetum hyemale*. *Planta* **163,** 350–359.

Favery B, Ryan E, Foreman J, Linstead P, Boudonck K, Steer M, Shaw P, Dolan L. 2001. *KOJAK* encodes a cellulose synthase-like protein required for root hair cell morphogenesis in *Arabidopsis*. *Genes and Development* **15,** 79–89.

Ferguson C, Teeri TT, Siika-aho M, Read SM, Bacic A. 1998. Location of cellulose and callose in pollen tubes and grains of *Nicotiana tabacum*. *Planta* **206,** 452–460.

Geitmann A, Steer M. 2006. The architecture and properties of the pollen tube cell wall. In: Malhó R, ed. *The pollen tube. Plant Cell Monographs*, Vol. 3. Berlin: Springer Verlag, 177–200.

Haigler CH, Brown RM. 1986. Transport of rosettes from the golgi apparatus to the plasma membrane in isolated mesophyll cells of *Zinnia elegans* during differentiation to tracheary elements in suspension culture. *Protoplasma* **134,** 111–120.

Hamann T, Osborne E, Youngs HL, Misson J, Nussaume L, Somerville C. 2004. Global expression analysis of *CESA* and *CSL* genes in Arabidopsis. *Cellulose* **11,** 279–286.

Hoch HC, Galvani CD, Szarowski DH, Turner JN. 2005. Two new fluorescent dyes applicable for visualization of fungal cell walls. *Mycologia* **97,** 580–588.

Honys D, Twell D. 2003. Comparative analysis of the Arabidopsis pollen transcriptome. *Plant Physiology* **132,** 640–652.

Honys D, Twell D. 2004. Transcriptome analysis of haploid male gametophyte development in. *Arabidopsis*. *Genome Biology* **5,** R85.

Hülskamp M, Schneitz K, Pruitt RE. 1995. Genetic evidence for a long-range activity that directs pollen tube guidance in *Arabidopsis*. *The Plant Cell* **7,** 57–64.

Jia DJ, Cao X, Wang W, Tan XY, Zhang XQ, Chen LQ, Ye D. 2009. *GNOM-LIKE 2,* encoding an adenosine diphosphate-ribosylation factor-guanine nucleotide exchange factor protein homologous to GNOM and GNL1, is essential for pollen germination in *Arabidopsis*. *Journal of Integrative Plant Biology* **51,** 762–773.

Jiang L, Yang SL, Xie LF, Puah CS, Zhang XQ, Yang WC, Sundaresan V, Ye D. 2005. *VANGUARD1* encodes a pectin methylesterase that enhances pollen tube growth in the Arabidopsis style and transmitting tract. *The Plant Cell* **17,** 584–596.

Johnson MA, Preuss D. 2002. Plotting a course: multiple signals guide pollen tubes to their targets. *Developmental Cell* **2,** 273–281.

Kim CM, Park SH, Je BI, Park SH, Park SJ, Piao HL, Eun MY, Dolan L, Han CD. 2007. *OsCSLD1*, a cellulose synthase-like D1 gene, is required for root hair morphogenesis in rice. *Plant Physiology* **143,** 1220–1230.

Kimura S, Laosinchai W, Itoh T, Cui X, Linder CR, Brown Jr. RM. 1999. Immunogold labeling of rosette terminal cellulose-synthesizing complexes in the vascular plant *Vigna angularis*. *The Plant Cell* **11,** 2075–2086.

Kurek I, Kawagoe Y, Jacob-Wilk D, Doblin M, Delmer D. 2002. Dimerization of cotton fiber cellulose synthase catalytic subunits occurs via oxidation of the zinc-binding domains. *Proceedings of the National Academy of Sciences, USA* **99,** 11109–11114.

Lancelle SA, Hepler PK. 1992. Ultrastructure of freeze-substituted pollen tubes of. *Lilium longiflorum*. *Protoplasma* **167,** 215–230.

Lee YJ, Szumlanski A, Nielsen E, Yang Z. 2008. Rho-GTPase-dependent filamentous actin dynamics coordinate vesicle targeting and exocytosis during tip growth. *Journal of Cell Biology* **181,** 1155–1168.

Lennon KA, Lord EM. 2000. *In vivo* pollen tube cell of *Arabidopsis thaliana* I. Tube cell cytoplasm and wall. *Protoplasma* **214,** 45–56.

Li H, Bacic A, Read SM. 1999*a*. Role of a callose synthase zymogen in regulating wall deposition in pollen tubes of *Nicotiana alata* Link et Otto. *Planta* **208,** 528–538.

Li H, Lin Y, Heath RM, Zhu MX, Yang Z. 1999*b*. Control of pollen tube tip growth by a Rop GTPase-dependent pathway that leads to tip-localized calcium influx. *The Plant Cell* **11,** 1731–1742.

Li M, Xiong G, Li R, Cui J, Tang D, Zhang B, Pauly M, Cheng Z, Zhou Y. 2009. Rice cellulose synthase-like D4 is essential for normal cell-wall biosynthesis and plant growth. *The Plant Journal* **60,** 1055–1069.

Liepman AH, Wilkerson CG, Keegstra K. 2005. Expression of cellulose synthase-like (*Csl*) genes in insect cells reveals that *CslA* family members encode mannan synthases. *Proceedings of the National Academy of Sciences, USA* **102,** 2221–2226.

Liu YG, Mitsukawa N, Oosumi T, Whittier RF. 1995. Efficient isolation and mapping of *Arabidopsis thaliana* T-DNA insert junctions by thermal asymmetric interlaced PCR. *The Plant Journal* **8,** 457–463.

Lord EM, Russell SD. 2002. The mechanisms of pollination and fertilization in plants. *Annual Review of Cell and Developmental Biology* **18,** 81–105.

McCormick S. 2004. Control of male gametophyte development. *The Plant Cell* **16 Suppl,** S142–S153.

Moscatelli A, Idilli AI. 2009. Pollen tube growth: a delicate equilibrium between secretory and endocytic pathways. *Journal of Integrative Plant Biology* **51,** 727–739.

Murashige T, Skoog F. 1962. A revised medium for rapid growth and bioassays with tobacco tissue cultures. *Physiologia Plantarum* **15,** 473–497.

Mutwil M, Debolt S, Persson S. 2008. Cellulose synthesis: a complex complex. *Current Opinion in Plant Biology* **11,** 252–257.

Natera SH, Ford KL, Cassin AM, Patterson JH, Newbigin EJ, Bacic A. 2008. Analysis of the *Oryza sativa* plasma membrane proteome using combined protein and peptide fractionation approaches in conjunction with mass spectrometry. *Journal of Proteome Research* **7,** 1159–1187.

Nishikawa S, Zinkl GM, Swanson RJ, Maruyama D, Preuss D. 2005. Callose (β-1,3 glucan) is essential for *Arabidopsis* pollen wall patterning, but not tube growth. *BMC Plant Biology* **5,** 22.

Paredez AR, Somerville CR, Ehrhardt DW. 2006. Visualization of cellulose synthase demonstrates functional association with microtubules. *Science* **312,** 1491–1495.

Persson S, Paredez A, Carroll A, Palsdottir H, Doblin M, Poindexter P, Khitrov N, Auer M, Somerville CR. 2007. Genetic evidence for three unique components in primary cell-wall cellulose synthase complexes in *Arabidopsis*. *Proceedings of the National Academy of Sciences, USA* **104,** 15566–15571.

Preuss D, Rhee SY, Davis RW. 1994. Tetrad analysis possible in *Arabidopsis* with mutation of the *QUARTET* (*QRT*) genes. *Science* **264,** 1458–1460.

Qin Y, Leydon AR, Manziello A, Pandey R, Mount D, Denic S, Vasic B, Johnson MA, Palanivelu R. 2009. Penetration of the stigma and style elicits a novel transcriptome in pollen tubes, pointing to genes critical for growth in a pistil. *PLoS Genetics* **5,** e1000621.

Reiss HD, Herth W, Schnepf E. 1985. Plasma-membrane 'rosettes' are present in the lily pollen tube. *Naturwissenschaften* **72,** 276.

Rhee SY, Somerville CR. 1998. Tetrad pollen formation in quartet mutants of *Arabidopsis thaliana* is associated with persistence of pectic polysaccharides of the pollen mother cell wall. *The Plant Journal* **15,** 79–88.

Richmond TA, Somerville CR. 2000. The cellulose synthase superfamily. *Plant Physiology* **124,** 495–498.

Roberts AW, Bushoven JT. 2007. The cellulose synthase (*CESA*) gene superfamily of the moss. *Physcomitrella patens*. *Plant Molecular Biology* **63,** 207–219.

Roberts AW, Roberts E. 2007. Evolution of the cellulose synthase (*CesA*) gene family: insights from green algae and seedless plants. In: Brown RM, Saxena IM, eds. *Cellulose: molecular and structural biology*. Dordrecht: Springer, 17–34.

Sauter M, Seagull RW, Kende H. 1993. Internodal elongation and orientation of cellulose microfibrils and microtubules in deepwater rice. *Planta* **190,** 354–362.

Schlüpmann H, Bacic A, Read SM. 1994. Uridine diphosphate glucose metabolism and callose synthesis in cultured pollen tubes of *Nicotiana alata* Link et Otto. *Plant Physiology* **105,** 659–670.

Smyth DR, Bowman JL, Meyerowitz EM. 1990. Early flower development in. *Arabídopsis*. *The Plant Cell* **2,** 755–767.

Song XF, Yang CY, Liu J, Yang WC. 2006. RPA, a class II ARFGAP protein, activates ARF1 and U5 and plays a role in root hair development in *Arabidopsis*. *Plant Physiology* **141,** 966–976.

Steer MW, Steer JM. 1989. Pollen tube tip growth. *New Phytologist* **111,** 323–358.

Sundaresan V, Springer P, Volpe T, Haward S, Jones JD, Dean C, Ma H, Martienssen R. 1995. Patterns of gene action in plant development revealed by enhancer trap and gene trap transposable elements. *Genes and Development* **9,** 1797–1810.

Szumlanski AL, Nielsen E. 2009. The Rab GTPase RabA4d regulates pollen tube tip growth in *Arabidopsis thaliana*. *The Plant Cell* **21,** 526–544.

Tan XY, Liu XL, Wang W, Jia DJ, Chen LQ, Zhang XQ, Ye D. 2010. Mutations in the *Arabidopsis* nuclear-encoded mitochondrial phage-type RNA polymerase gene *RPOTm* led to defects in pollen tube growth, female gametogenesis and embryogenesis. *Plant and Cell Physiology* **51,** 635–649.

Taylor NG. 2008. Cellulose biosynthesis and deposition in higher plants. *New Phytologist* **178,** 239–252.

Taylor NG, Howells RM, Huttly AK, Vickers K, Turner SR. 2003. Interactions among three distinct CesA proteins essential for cellulose synthesis. *Proceedings of the National Academy of Sciences, USA* **100,** 1450–1455.

Tsekos I. 1999. The sites of cellulose synthesis in algae: diversity and evolution of cellulose-synthesizing enzyme complexes. *Journal of Phycology* **35,** 635–655.

Tsekos I, Reiss HD. 1994. Tip cell growth and the frequency and distribution of cellulose microfibril-synthesizing complexes in the plasma membrane of apical shoot cells of the red alga *Porphyra yezoensis*. *Journal of Phycology* **30,** 300–310.

Wada M, Staehelin LA. 1981. Freeze-fracture observations on the plasma membrane, the cell wall and the cuticle of growing protonemata of *Adiantum capillus-veneris* L. *Planta* **151,** 462–468.

Wang X, Cnops G, Vanderhaeghen R, De Block S, Van Montagu M, Van Lijsebettens M. 2001. *AtCSLD3*, a cellulose synthase-like gene important for root hair growth in Arabidopsis. *Plant Physiology* **126,** 575–586.

Yang SL, Xie LF, Mao HZ, Puah CS, Yang WC, Jiang L, Sundaresan V, Ye D. 2003. *Tapetum determinant1* is required for cell specialization in the Arabidopsis anther. *The Plant Cell* **15,** 2792–2804.

Yang WC, Ye D, Xu J, Sundaresan V. 1999. The *SPOROCYTELESS* gene of *Arabidopsis* is required for initiation of sporogenesis and encodes a novel nuclear protein. *Genes and Development* **13,** 2108–2117.

Yin Y, Huang J, Xu Y. 2009. The cellulose synthase superfamily in fully sequenced plants and algae. *BMC Plant Biology* **9,** 99.

Zinkl GM, Zwiebel BI, Grier DG, Preuss D. 1999. Pollen–stigma adhesion in *Arabidopsis*: a species-specific interaction mediated by lipophilic molecules in the pollen exine. *Development* **126,** 5431–5440.